

## Short Communication

## Hydrogen production from ammonia using a microwave plasma torch at atmospheric pressure

R. Antunes<sup>a</sup>, A. Meindl<sup>a</sup>, C. Kranig<sup>a</sup>, A. Hecimovic<sup>a</sup>, U. Fantz<sup>a,b</sup><sup>a</sup> Max Planck Institute for Plasma Physics, Boltzmannstraße 2, Garching b. München, 85748, Germany<sup>b</sup> AG Experimentelle Plasmaphysik, University of Augsburg, Augsburg, 86135, Germany

## ARTICLE INFO

## Keywords:

Ammonia dissociation  
Hydrogen production  
Hydrogen storage  
MW plasma torch

## ABSTRACT

An electrodeless, catalyst-free microwave (MW) plasma torch has been investigated to produce hydrogen ( $H_2$ ) from ammonia ( $NH_3$ ) dissociation, with  $NH_3$  admixed in nitrogen up to 90 vol.% using a total inlet flow rate of 10 sLm at atmospheric pressure. Conversions beyond 99% are obtained for MW powers between 1.50–1.75 kW. The largest  $H_2$  energy yield  $\approx 447 L_{H_2} kWh^{-1}$ , or lowest energy cost of  $25 kWh kg_{H_2}^{-1}$ , is obtained for 90 vol.% [ $NH_3$ ], which corresponds to outlet concentrations of  $H_2$  and  $NH_3$  around 69 vol.% and below 1 vol.%, respectively. These performances are highly promising for the application of plasma technology for the production of hydrogen from ammonia.

## 1. Introduction

Hydrogen ( $H_2$ ) production from ammonia ( $NH_3$ ), for example to be used to feed fuel cells for power generation [1,2], has received strong interest from the scientific community and industry.  $NH_3$  is a carbon-free molecule, it has high volumetric energy density (around  $10 MJ L^{-1}$ , comparable to compressed natural gas and methanol) as well as high hydrogen storage capacity (17.8 wt.%), and a worldwide infrastructure for ammonia transportation already exists [3,4]. Ammonia dissociation is an endothermic reaction ( $2NH_3 \rightarrow N_2 + 3H_2$ ,  $\Delta H = +91.88 kJ mol^{-1}$  [5]), thermodynamically favoured at high temperatures and low pressures [6]. The thermal decomposition of ammonia is enhanced in presence of catalysts, the most active of which are ruthenium-based [7,8]. Despite its high activity for ammonia dissociation, ruthenium is an expensive metal, which requires the need to develop alternative, cheaper catalysts that enable complete dissociation at low-to-moderate temperatures ( $\approx 650 K$ ) [9,10]. Complete conversion of pure ammonia flowing through a catalytic reactor would result in 75 vol.% of  $H_2$  in the outlet stream, which makes the use of downstream separation/purification steps necessary. An example where high-purity  $H_2$  streams (above 99.9 vol.%) from  $NH_3$  cracking are achieved is with catalytic membrane reactors, in which palladium-based membranes allow the in-situ extraction of  $H_2$  by permeation [11,12].

Plasma conversion technology, owing to its inherent compatibility with intermittent electricity, highly reactive environment, tunable selectivity, and wide range of gas temperatures can be a promising route to produce  $H_2$  from  $NH_3$ . Non-thermal dielectric barrier discharges,

due to the acceptable surface temperatures, allow increasing conversions by placing the plasma in contact with a catalyst at atmospheric pressure. For instance, Wang et al. reported an increase in conversion from around 7.8% with plasma alone to 99.9% using an iron-based catalyst in presence of plasma at 683 K [13]. Rotating gliding arcs, which are discharges that favour gas temperatures of several thousand kelvin, have been reported to achieve conversions of 80% without catalyst, albeit with large uncertainties due to a significant erosion of the electrode used in this plasma process [14]. Microwave (MW) plasmas are sources that also yield high gas temperatures with relatively high gas throughputs and in principle do not require electrodes. MW plasma torches, which have been mainly studied for the endothermic reaction of  $CO_2$  dissociation by different groups, yield thermal plasmas at atmospheric pressure with gas temperatures at around 6000 K [15–18]. These sources enable large conversions for  $CO_2$  and their relative flexibility and ease of operation motivate its use towards other endothermic reactions such as  $NH_3$  cracking. Recently, a microwave plasma torch has been studied for the dissociation of ammonia admixed with nitrogen for which gas temperatures between 5000 and 6000 K and conversions of 65–85% for relatively low ammonia concentrations in the feed gas (17 to 42 vol.%  $NH_3/N_2$ ) are reported [19].

This short communication aims at reporting very large conversions beyond 99% obtained with a microwave plasma torch at atmospheric pressure without catalyst and with gas mixtures up to 90 vol.%  $NH_3$  in  $N_2$ .

\* Corresponding author.

E-mail address: [rodrigo.antunes@ipp.mpg.de](mailto:rodrigo.antunes@ipp.mpg.de) (R. Antunes).<https://doi.org/10.1016/j.ijhydene.2025.151121>

Received 1 July 2025; Received in revised form 12 August 2025; Accepted 21 August 2025

Available online 30 August 2025

0360-3199/© 2025 The Authors. Published by Elsevier Ltd on behalf of Hydrogen Energy Publications LLC. This is an open access article under the CC BY-NC-ND license (<http://creativecommons.org/licenses/by-nc-nd/4.0/>).

## 2. Experimental

Fig. 1 displays the experimental setup used in this work. The microwave plasma torch consists of four tangential gas inlets at the bottom (inner diameter 1.5 mm), a coaxial (pin) and cylindrical resonators. The tangential inlets produce a gas flow that swirls inside a quartz tube (140 mm long, 30 mm wide, 2 mm wall thickness), which is sealed on the bottom to the resonator and connected on the top to a water-cooled stainless steel piece by O-rings. The plasma is ignited by coupling 2.45 GHz, magnetron-generated microwaves through a three-stub tuner (SAIREM, GMP G4 60K, 6 kW of nominal power) and the hot effluent gas is cooled down through a 2 m long heat exchanger. The cold gas is sampled to a quadrupole mass spectrometer (MS, Pfeiffer Vacuum, QMG 220 PrismaPlus) for gas composition analysis, calibrated for  $\text{NH}_3$ ,  $\text{N}_2$  and  $\text{H}_2$  following the procedure described in [20]. The whole setup is connected to a vacuum pump (Leybold, TRIVAC D16B) to ensure safe operation at quasi-atmospheric pressure ( $\approx 940$  mbar), which is equivalent to operation at atmospheric pressure as demonstrated in a previous work [21]. The base pressure of the entire setup is  $\leq 10^{-1}$  mbar and the pressure inside the reactor (measured by Pfeiffer Vacuum, PCR 280) is regulated by a bellows valve. Nitrogen (5.0 purity, Air Liquide) and ammonia (5.0 purity, Air Liquide) are injected into the reactor by means of mass-flow controllers (Brooks Instrument, GF40). With the setup used in this work, the discharge is first initiated at around 100 mbar with pure  $\text{N}_2$ , and  $\text{NH}_3$  is injected at elevated pressures until the desired composition is reached. The pure  $\text{N}_2$  plasma is characterized by a pink column, which is characteristic of the intense  $\text{N}_2^+$  first negative system emission in these types of sources [22]. The visible column shrinks with the addition of  $\text{NH}_3$  and at large  $[\text{NH}_3]$  a yellow glow forms around it and extends beyond the top of the resonator (Fig. 1b). This glow is attributed to the emission of  $\text{NH}_2^+$  [19]. The experiments are carried out at  $\approx 940$  mbar and with a total inlet flow rate of  $F_{\text{total},\text{in}} = 10$  sLm (sLm: standard Liter per minute at 273.15 K, 1013 mbar). With the increase of  $[\text{NH}_3]$  in the plasma, a larger power is required to sustain it. For 10–90 vol.%  $[\text{NH}_3]$ , the net MW plasma power (given by  $P_{\text{MW},\text{net}} = P_{\text{MW},\text{forward}} - P_{\text{MW},\text{reflected}}$ ) was varied between 1.0 and 1.75 kW. The only molecules detected in the effluent are  $\text{NH}_3$ ,  $\text{H}_2$  and  $\text{N}_2$  and their concentrations are determined by averaging  $\approx 15$  min of constant MS current signals and the standard deviation used for their uncertainty.

To quantify the performance of the MW plasma torch, two key parameters, the  $\text{NH}_3$  conversion  $\chi_{\text{NH}_3}$  defined by Eq. (1) and the  $\text{H}_2$  energy yield  $Y_{\text{H}_2}$  in  $\text{L}_{\text{H}_2} \text{ kWh}^{-1}$  given by (2), are used.  $[\text{NH}_3]_{\text{in}}$  and  $[\text{NH}_3]_{\text{out}}$  are the ammonia concentrations at the inlet and outlet, respectively.  $F_{\text{H}_2,\text{out}}$  is the total hydrogen outflow rate in sLm,  $[\text{H}_2]_{\text{out}}$  is the outlet concentration of  $\text{H}_2$  and  $F_{\text{total},\text{out}}$  is the total outflow rate, calculated by:  $F_{\text{total},\text{out}} = F_{\text{N}_2,\text{in}} + (1 + \chi_{\text{NH}_3})F_{\text{NH}_3,\text{in}}$ , with  $F_{\text{N}_2,\text{in}}$  and  $F_{\text{NH}_3,\text{in}}$  being the total inlet flow rates of  $\text{N}_2$  and  $\text{NH}_3$  in sLm, respectively. Note that for  $\chi_{\text{NH}_3} = 1$ ,  $F_{\text{total},\text{out}} = F_{\text{N}_2,\text{in}} + 2F_{\text{NH}_3,\text{in}}$  which accounts for gas expansion upon dissociation of 1 mol of  $\text{NH}_3$  into 0.5 mol of  $\text{N}_2$  and 1.5 mol of  $\text{H}_2$ . The uncertainties for  $\chi_{\text{NH}_3}$  and  $Y_{\text{H}_2}$  are determined by propagating the uncertainties for the concentrations and flow rates.

$$\chi_{\text{NH}_3} = \frac{1 - \frac{[\text{NH}_3]_{\text{out}}}{[\text{NH}_3]_{\text{in}}}}{1 + \frac{[\text{NH}_3]_{\text{out}}}{[\text{NH}_3]_{\text{in}}}} \quad (1)$$

$$Y_{\text{H}_2} = \frac{F_{\text{H}_2,\text{out}}}{P_{\text{MW},\text{net}}} \times 60 = [\text{H}_2]_{\text{out}} \frac{F_{\text{total},\text{out}}}{P_{\text{MW},\text{net}}} \times 60 \quad (2)$$

## 3. Results and discussion

Conversions above 99% have been achieved for 50–80 vol.%  $\text{NH}_3$  in  $\text{N}_2$  with an electrodeless and catalyst-free microwave plasma torch, as displayed in Fig. 2a. With the increase of the ammonia concentration in the feed gas, a larger MW power is required to promote high conversions. A clear example of this is the drop in conversion from 98.9% to

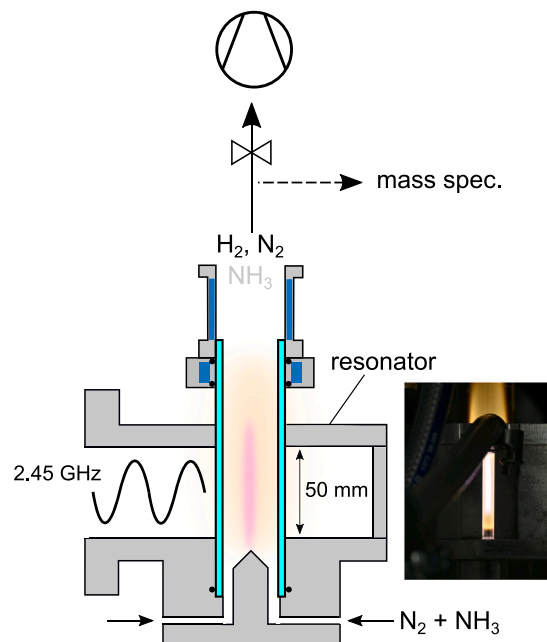


Fig. 1. Experimental setup (a.) and photo of the discharge with 40 vol.%  $\text{NH}_3$  in  $\text{N}_2$  with  $P_{\text{net}} = 1.00$  kW (b.).

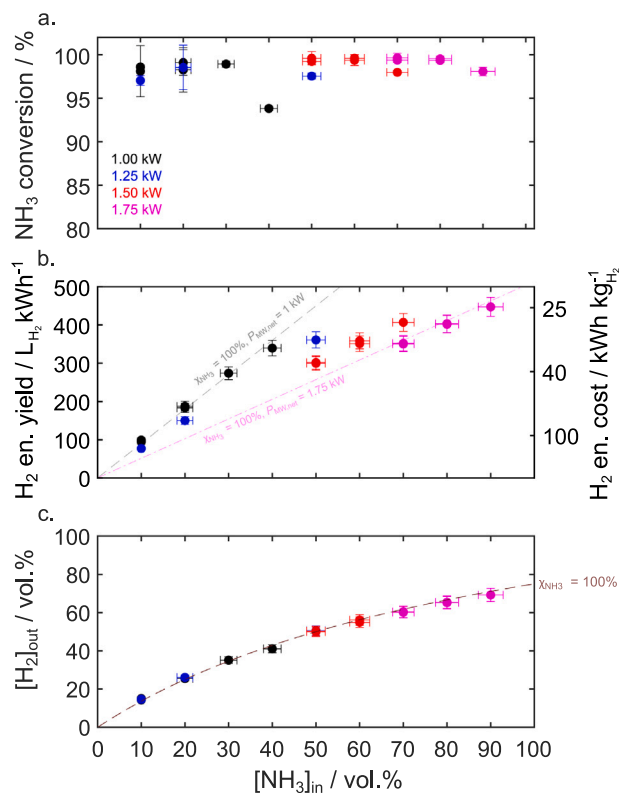
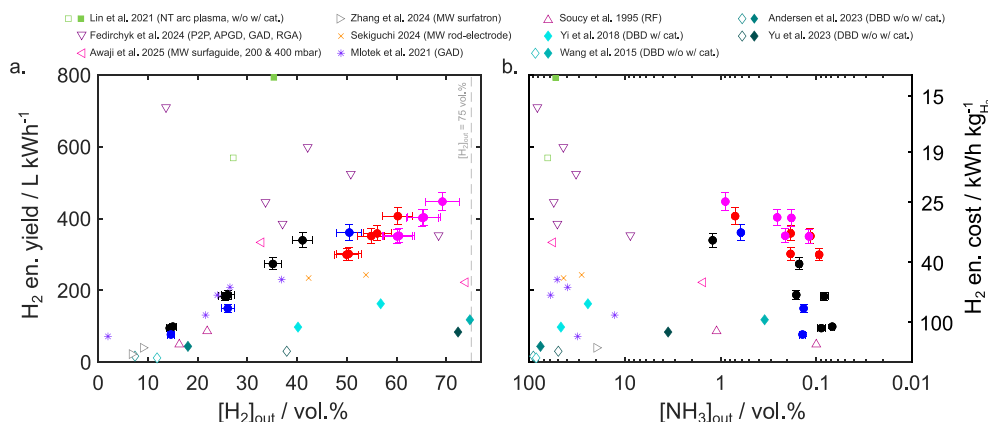


Fig. 2. Ammonia conversion (a.),  $\text{H}_2$  energy yield (b.) and  $[\text{H}_2]_{\text{out}}$  (c.) as a function of the ammonia inlet concentration in nitrogen. Black circles:  $P_{\text{MW},\text{net}} = 1.00$  kW; blue circles:  $P_{\text{MW},\text{net}} = 1.25$  kW; red circles  $P_{\text{MW},\text{net}} = 1.50$  kW; magenta circles:  $P_{\text{MW},\text{net}} = 1.75$  kW. Total flow rate:  $F_{\text{total},\text{out}} = 10$  sLm. (For interpretation of the references to colour in this figure legend, the reader is referred to the web version of this article.)



**Fig. 3.** H<sub>2</sub> energy yield as a function [H<sub>2</sub>]<sub>out</sub> (a.) and [NH<sub>3</sub>]<sub>out</sub> (b.) compared with literature data: Lin et al. [23], Fedirchik et al. [14], Awaji et al. [24], Zhang et al. [25], Sekiguchi et al. [26], Mlotek et al. [27], Soucy et al. [28], Yi et al. [29], Wang et al. [30], Andersen et al. [31], Yu et al. [32]. P2P: pin-to-pin, APGD: atmospheric pressure glow discharge, GAD: gliding arc, RGA: rotating gliding arc, DBD: dielectric barrier discharge. Unless stated otherwise, all data points were obtained at atmospheric pressure. The circles correspond to the values presented in Fig. 2. (For interpretation of the references to colour in this figure legend, the reader is referred to the web version of this article.)

93.8% when increasing the ammonia content from 30 to 40 vol.% with 1 kW. With larger ammonia concentrations, MW powers of 1.50 kW and 1.75 kW enable conversions above 99%. The decrease in conversion from 99.5% to 98% with the increase of [NH<sub>3</sub>] from 80 to 90 vol.% suggests that powers above 1.75 kW are needed to maintain higher conversions. The large conversions translate into H<sub>2</sub> energy yields close to the theoretical maximum at a given power. This can be appreciated in Fig. 2b, in which the H<sub>2</sub> yields obtained with 1.0 kW and 1.75 kW closely follow the values for 100% dissociation and the same applies for the other microwave powers. In general, an increase in [NH<sub>3</sub>]<sub>in</sub> allows an increase in energy yield. However, note that, although an increase in power results in larger conversions, it can also lead to a reduction of the energy yield, as for example for 50 and 70 vol.% [NH<sub>3</sub>]<sub>in</sub>. The largest energy yield  $\approx 447 \text{ L kWh}^{-1}$  is obtained at 90 vol.% [NH<sub>3</sub>]<sub>in</sub>, corresponding to an energy cost of  $25 \text{ kWh kg}_{\text{H}_2}^{-1}$ . The concentration of H<sub>2</sub> at the outlet of reactor must be considered as well and it can be appreciated in Fig. 2c that the [H<sub>2</sub>]<sub>out</sub> values lie close to the maximum values that can be achieved for each gas composition. The largest [H<sub>2</sub>]<sub>out</sub> is around 69 vol.%, which is remarkable considering that the highest possible concentration corresponding to 100% dissociation with pure NH<sub>3</sub> is 75 vol.% [H<sub>2</sub>]<sub>out</sub>.

The results displayed in Fig. 2a suggest that the amount of dissociated ammonia is dependent on the energy delivered per ammonia molecule, or specific energy input. However, the increase of the net MW power can also have a direct impact on the conversion, for instance by increasing the gas temperature in the effluent, which contributes to further dissociation of NH<sub>3</sub>. Such a direct impact between the microwave power and gas effluent temperatures has been previously reported for CO<sub>2</sub> plasmas using this plasma torch [33,34]. Moreover, the increase in MW power is expected to yield larger electron densities in the plasma, which may enable further dissociation of NH<sub>3</sub> by electron-impact dissociation. Indeed, Niu et al. reported an increase in emission of excited N<sub>2</sub><sup>+</sup> and NH from the plasma core with the increase of MW plasma power [19]. Further insights about the plasma chemistry can be gained with optical emission spectroscopy, which will be used in the future to investigate gas temperatures and electron densities under relevant conditions. The limitation on the maximum [NH<sub>3</sub>] concentration of 90 vol.% and maximum power of 1.75 kW is imposed by the heat management of the current plasma torch resonator. A similar limitation was encountered in plasma conversion of CO<sub>2</sub> molecule, which has been resolved by using a reverse vortex and fast cooling of the effluent gas [17]. Similar approaches focused on the heat management are envisaged as a next step towards removing the limits on the maximum ammonia concentration and microwave power.

Contrary to its impact on the conversion of CO<sub>2</sub>, fast cooling is not expected to affect ammonia decomposition, whose stable dissociation products (mainly N<sub>2</sub>, with its triple bond and dissociation energy of  $945 \text{ kJ mol}^{-1}$  [35]) are very unlikely to react back to form NH<sub>3</sub> at atmospheric pressure. As discussed by Fedirchik et al. gas quenching in ammonia plasmas will likely not improve conversions [14].

For the application of plasmas for hydrogen production it is most relevant to consider the energy used to produce a given amount of H<sub>2</sub> (i.e. the H<sub>2</sub> energy yield) and the outlet concentrations of H<sub>2</sub> and NH<sub>3</sub>. While high H<sub>2</sub> purities ( $\geq 99.97 \text{ vol.}\%$ ) are required for fuel cells in road vehicles [36], the presence of NH<sub>3</sub> in the feed gas at concentrations as low as 0.1 ppm has a negative effect on fuel cell operation [1]. Consequently, a downstream separation/purification system is required and its size is directly impacted by the gas composition at the outlet of the reactor. It should be pointed out that N<sub>2</sub> is also an undesired impurity, but, apart from diluting the incoming hydrogen, it does not have a degrading effect [37]. The energy yields obtained in this work are plotted in Fig. 3 as a function of both [H<sub>2</sub>]<sub>out</sub> and [NH<sub>3</sub>]<sub>out</sub> and compared to results reported in the literature (note the inverted x-scale in Fig. 3b). Large energy yields as high as  $800 \text{ L}_{\text{H}_2} \text{ kWh}^{-1}$  have been reported by Lin et al. using a non-thermal arc plasma with a NiO/Al<sub>2</sub>O<sub>3</sub> catalyst [23], however with only 35 vol.% H<sub>2</sub> at the outlet. Another interesting example is the H<sub>2</sub> energy yield of  $524 \text{ L}_{\text{H}_2} \text{ kWh}^{-1}$  reported by Fedirchik et al. using a gliding arc plasma [14], albeit with an outlet stream containing [H<sub>2</sub>]<sub>out</sub> = 51 vol.% and [NH<sub>3</sub>]<sub>out</sub> = 32 vol.%. Overall, the results reported so far seem to suggest a trade-off between the H<sub>2</sub> energy yield and [NH<sub>3</sub>]<sub>out</sub> (Fig. 3b), while the MW plasma torch enables relatively large yields for [NH<sub>3</sub>]<sub>out</sub>  $\lesssim 1 \text{ vol.}\%$ .

Energy costs for H<sub>2</sub> production from NH<sub>3</sub> cracking using thermo-catalytic processes lie in the range of  $6 - 16 \text{ kWh kg}_{\text{H}_2}^{-1}$  [38] and around  $9 \text{ kWh kg}_{\text{H}_2}^{-1}$  for electrochemical conversion [39], placing these technologies closer to the thermodynamic limit of  $4.2 \text{ kWh kg}_{\text{H}_2}^{-1}$ . However, the results presented here demonstrate that reduction in energy costs by further increase of NH<sub>3</sub> flow rates at increased MW powers should be expected. Further improvements in the process efficiency could be achieved by implementation of heat recovery strategies. By eliminating the need of catalysts and electrodes, the MW plasma torch presents a promising advantage for sustained, long-term use.

#### 4. Conclusions

A microwave-drive plasma torch operated without electrodes or catalyst materials has been studied for the decomposition of NH<sub>3</sub> mixed in N<sub>2</sub> up to 90 vol.%. Very high conversions exceeding 99% have been

obtained for 50 – 80 vol.% of ammonia in the feed gas. At 90 vol.%  $\text{NH}_3$  the conversion slightly decreases to 98% for a MW power of 1.75 kW, corresponding to a hydrogen yield of  $\approx 447 \text{ L}_{\text{H}_2} \text{ kWh}^{-1}$  or an energy cost of  $25 \text{ kWh kg}_{\text{H}_2}^{-1}$ , and outlet concentrations of 69 vol.%  $\text{H}_2$  and  $\leq 1 \text{ vol.}\%$   $\text{NH}_3$ . Future work will include gaining insights into the plasma chemistry by spectroscopic methods and improvements to the reactor design to cope with the high gas effluent temperatures.

### CRediT authorship contribution statement

**R. Antunes:** Writing – review & editing, Writing – original draft, Validation, Methodology, Investigation, Formal analysis, Data curation, Conceptualization. **A. Meindl:** Writing – review & editing, Investigation. **C. Kranig:** Writing – review & editing, Investigation. **A. Hecimovic:** Writing – review & editing, Resources, Project administration, Funding acquisition. **U. Fantz:** Writing – review & editing, Resources, Project administration, Funding acquisition.

### Declaration of competing interest

The authors declare that they have no known competing financial interests or personal relationships that could have appeared to influence the work reported in this paper.

### References

- [1] Chiuta S, Everson RC, Neomagus HW, van der Gryp P, Bessarabov DG. Reactor technology options for distributed hydrogen generation via ammonia decomposition: A review. *Int J Hydrog Energy* 2013;38(35):14968–91. <http://dx.doi.org/10.1016/j.ijhydene.2013.09.067>.
- [2] Yan J, Wang J, Cai S, Zang C, Li S, Tu Z. Comprehensive evaluation of proton exchange membrane fuel cell-based power system fueled with ammonia decomposed hydrogen. *Int J Hydrog Energy* 2025;140:853–69. <http://dx.doi.org/10.1016/j.ijhydene.2025.01.480>.
- [3] Kobayashi H, Hayakawa A, Somarathne KKA, Okafor EC. Science and technology of ammonia combustion. *Proc Combust Inst* 2019;37(1):109–33. <http://dx.doi.org/10.1016/j.proci.2018.09.029>.
- [4] IRENA. Global hydrogen trade to meet the 1.5° C climate goal: Part II – Technology review of hydrogen carriers. Technical report, Abu Dhabi: International Renewable Energy Agency; 2022.
- [5] Chase M. NIST-JANAF thermochemical tables. 4th ed. American Institute of Physics; 1998.
- [6] Lucentini I, Garcia X, Vendrell X, Llorca J. Review of the decomposition of ammonia to generate hydrogen. *Ind Eng Chem Res* 2021;60(51):18560–611. <http://dx.doi.org/10.1021/acs.iecr.1c00843>.
- [7] Hill AK, Torrente-Murciano L. Low temperature  $\text{H}_2$  production from ammonia using ruthenium-based catalysts: Synergetic effect of promoter and support. *Appl Catal B: Environ* 2015;172–173:129–35. <http://dx.doi.org/10.1016/j.apcatb.2015.02.011>.
- [8] Su Z, Guan J, Liu Y, Shi D, Wu Q, Chen K, et al. Research progress of ruthenium-based catalysts for hydrogen production from ammonia decomposition. *Int J Hydrog Energy* 2024;51:1019–43. <http://dx.doi.org/10.1016/j.ijhydene.2023.09.107>.
- [9] Schüth F, Palkovits R, Schlögl R, Su DS. Ammonia as a possible element in an energy infrastructure: catalysts for ammonia decomposition. *Energy Env Sci* 2012;5(4):6278–89. <http://dx.doi.org/10.1039/c2ee02865d>.
- [10] Zhang M, Wen J, Zhang Y, Wu Y, Zhao Z, Yan J, et al. Advances in the development of ammonia decomposition to CO-free hydrogen: Catalyst materials and activity optimization. *Int J Hydrog Energy* 2025;102:571–93. <http://dx.doi.org/10.1016/j.ijhydene.2024.12.496>.
- [11] Cechetto V, Di Felice L, Medrano JA, Makhoulouf C, Zuniga J, Gallucci F.  $\text{H}_2$  production via ammonia decomposition in a catalytic membrane reactor. *Fuel Process Technol* 2021;216:106772. <http://dx.doi.org/10.1016/j.fuproc.2021.106772>.
- [12] Omata K, Yoshinaga H, Nambu T. Design and development of a novel membrane reactor assembled with a flat-plate hydrogen-permeable membrane and an ammonia decomposition catalyst for producing hydrogen from ammonia. *Int J Hydrog Energy* 2025;140:608–16. <http://dx.doi.org/10.1016/j.ijhydene.2025.05.281>.
- [13] Wang L, Zhao Y, Liu C, Gong W, Guo H. Plasma driven ammonia decomposition on a Fe-catalyst: eliminating surface nitrogen poisoning. *Chem Commun* 2013;49(36):3787. <http://dx.doi.org/10.1039/c3cc41301b>.
- [14] Fedirchuk I, Tsonev I, Quiroz Marnef R, Bogaerts A. Plasma-assisted  $\text{NH}_3$  cracking in warm plasma reactors for green  $\text{H}_2$  production. *Chem Eng J* 2024;499:155946. <http://dx.doi.org/10.1016/j.cej.2024.155946>.
- [15] D'Isa FA, Carbone EAD, Hecimovic A, Fantz U. Performance analysis of a 2.45 GHz microwave plasma torch for  $\text{CO}_2$  decomposition in gas swirl configuration. *Plasma Sources Sci Technol* 2020;29(10):105009. <http://dx.doi.org/10.1088/1361-6595/abaa84>.
- [16] Wiegiers K, Schulz A, Walker M, Tovar GEM. Determination of the conversion and efficiency for  $\text{CO}_2$  in an atmospheric pressure microwave plasma torch. *Chem Ing Tech* 2022;94(3):299–308. <http://dx.doi.org/10.1002/cite.202100149>.
- [17] Belov I, Vermeiren V, Paulussen S, Bogaerts A. Carbon dioxide dissociation in a microwave plasma reactor operating in a wide pressure range and different gas inlet configurations. *J CO2 Util* 2018;24:386–97. <http://dx.doi.org/10.1016/j.jcou.2017.12.009>.
- [18] van de Steeg A, Viegas P, Silva A, Butterworth T, van Bavel A, Smits J, et al. Redefining the microwave plasma-mediated  $\text{CO}_2$  reduction efficiency limit: The role of O– $\text{CO}_2$  association. *ACS Energy Lett* 2021;6(8):2876–81. <http://dx.doi.org/10.1021/acseenergylett.1c01206>.
- [19] Niu Y-L, Li S-Z, Wang X-C, Yu Q-K, Yang D, Wen X, et al. Characteristic study of nitrogen microwave plasma decomposition of ammonia at atmospheric pressure for hydrogen production. *Plasma Sources Sci Technol* 2024;33(10):105018. <http://dx.doi.org/10.1088/1361-6595/ad7ea4>.
- [20] Hecimovic A, D'Isa F, Carbone E, Drenik A, Fantz U. Quantitative gas composition analysis method for a wide pressure range up to atmospheric pressure— $\text{CO}_2$  plasma case study. *Rev Sci Instrum* 2020;91(11):113501. <http://dx.doi.org/10.1063/5.0013413>.
- [21] Kiefer CK, Antunes R, Hecimovic A, Meindl A, Fantz U.  $\text{CO}_2$  dissociation using a lab-scale microwave plasma torch: An experimental study in view of industrial application. *Chem Eng J* 2024;481:148326. <http://dx.doi.org/10.1016/j.cej.2023.148326>.
- [22] Li S-Z, Zhang X, Chen C-J, Zhang J, Wang Y-X, Xia G-Q. The quenching effect of hydrogen on the nitrogen in metastable state in atmospheric-pressure  $\text{N}_2\text{-H}_2$  microwave plasma torch. *Phys Plasmas* 2014;21(7). <http://dx.doi.org/10.1063/1.4891664>.
- [23] Lin Q, Jiang Y, Liu C, Chen L, Zhang W, Ding J, et al. Instantaneous hydrogen production from ammonia by non-thermal arc plasma combining with catalyst. *Energy Rep* 2021;7:4064–70. <http://dx.doi.org/10.1016/j.egyr.2021.06.087>.
- [24] Awaji M, Pentecoste-Cuyntet L, Noël C, Gries T, Belmahi M, Belmoute T. Ammonia cracking by microwave plasma under reduced pressure. *Int J Hydrog Energy* 2025;119:377–85. <http://dx.doi.org/10.1016/j.ijhydene.2025.03.118>.
- [25] Zhang X, Cha MS. Optimizing ammonia cracking in microwave argon plasma: Temperature control and ammonia delivery. *Chem Eng J* 2024;496:154289. <http://dx.doi.org/10.1016/j.cej.2024.154289>.
- [26] Sekiguchi H. Pure ammonia direct decomposition using rod-electrode-type microwave plasma source. *Int J Hydrog Energy* 2024;57:1010–6. <http://dx.doi.org/10.1016/j.ijhydene.2023.12.296>.
- [27] Miš otek M, Perron M, Krawczyk K. Ammonia decomposition in a gliding discharge plasma. *Energy Technol* 2021;9(12). <http://dx.doi.org/10.1002/ente.202100677>.
- [28] Soucy G, Jurewicz JW, Boulous MI. Parametric study of the decomposition of  $\text{NH}_3$  for an induction plasma reactor design. *Plasma Chem Plasma Process* 1995;15(4):693–710. <http://dx.doi.org/10.1007/bf01447067>.
- [29] Yi Y, Wang L, Guo Y, Sun S, Guo H. Plasma-assisted ammonia decomposition over Fe–Ni alloy catalysts for  $\text{CO}_2$ -free hydrogen. *AIChE J* 2018;65(2):691–701. <http://dx.doi.org/10.1002/aic.16479>.
- [30] Wang L, Yi Y, Zhao Y, Zhang R, Zhang J, Guo H.  $\text{NH}_3$  decomposition for  $\text{H}_2$  generation: Effects of cheap metals and supports on plasma-catalyst synergy. *ACS Catal* 2015;5(7):4167–74. <http://dx.doi.org/10.1021/acscatal.5b00728>.
- [31] Andersen J, Christensen J, Østberg M, Bogaerts A, Jensen A. Plasma-catalytic ammonia decomposition using a packed-bed dielectric barrier discharge reactor. *Int J Hydrog Energy* 2022;47(75):32081–91. <http://dx.doi.org/10.1016/j.ijhydene.2022.07.102>.
- [32] Yu X, Hu K, Zhang H, He G, Xia Y, Deng M, et al. Plasma-catalytic ammonia decomposition for carbon-free hydrogen production using low pressure-synthesized  $\text{Mo}_n$  catalyst. *Plasma Chem Plasma Process* 2022;43(1):183–97. <http://dx.doi.org/10.1007/s11090-022-10282-y>.
- [33] Antunes R, Wiegiers K, Hecimovic A, Kiefer CK, Buchberger S, Meindl A, et al. Proof of concept for  $\text{O}_2$  removal with multiple LCCF membranes accommodated in the effluent of a  $\text{CO}_2$  plasma torch. *ACS Sustain Chem Eng* 2023;11(44):15984–93. <http://dx.doi.org/10.1021/acssuschemeng.3c04862>.
- [34] Van Alphen S, Hecimovic A, Kiefer CK, Fantz U, Snyders R, Bogaerts A. Modelling post-plasma quenching nozzles for improving the performance of  $\text{CO}_2$  microwave plasmas. *Chem Eng J* 2023;462:142217. <http://dx.doi.org/10.1016/j.cej.2023.142217>.
- [35] Frost DC, McDowell CA. The dissociation energy of the nitrogen molecule. *Proc R Soc Lond Ser A. Math Phys Sci* 1956;236(1205):278–84. <http://dx.doi.org/10.1098/rspa.1956.0135>.
- [36] Yáñez M, Relvas F, Ortiz A, Gorri D, Mendes A, Ortiz I. PSA purification of waste hydrogen from ammonia plants to fuel cell grade. *Sep Purif Technol* 2020;240:116334. <http://dx.doi.org/10.1016/j.seppur.2019.116334>.
- [37] Wang X, Baker P, Zhang X, Garces HF, Bonville LJ, Pasaogullari U, et al. An experimental overview of the effects of hydrogen impurities on polymer electrolyte membrane fuel cell performance. *Int J Hydrog Energy* 2014;39(34):19701–13. <http://dx.doi.org/10.1016/j.ijhydene.2014.09.151>.

- [38] Staudt C, Hofsaß C, von Lewinski B, Mörs F, Prabhakaran P, Bajohr S, et al. Process engineering analysis of transport options for green hydrogen and green hydrogen derivatives. *Energy Technol* 2024;13(2). <http://dx.doi.org/10.1002/ente.202301526>.
- [39] Zhang K, Han Y, Zhao Y, Wei T, Fu J, Ren Z, et al. Energy-efficient and cost-effective ammonia electrolysis for converting ammonia to green hydrogen. *Cell Rep Phys Sci* 2024;5(9):102171. <http://dx.doi.org/10.1016/j.xcrp.2024.102171>.